Chapter

Ionothermal Synthesis of Metal-Organic Framework

Hyun-Chang Oh, Sukwoo Jung, Il-Ju Ko and Eun-Young Choi

Abstract

Ionothermal synthesis employs ionic liquids for synthesis of metal organic frameworks (MOFs) as solvent and template. The cations and anions of ionic liquids may be finely adjusted to produce a great variety of reaction environments and thus frameworks. Organisation of the structures synthesised from related ionic liquid combinations give rise to provocative chemical trends that may be used to predict future outcomes. Further analysis of their structures is possible by reducing the complex framework to its underlying topology, which by itself brings more precision to prediction. Through reduction, many seemingly different, but related classes of structures may be merged into larger groups and provide better understanding of the nanoscopic structures and synthesis conditions that gave rise to them. Ionothermal synthesis has promised to enable us to effectively plan the synthesis ahead for a given purpose. However, for its promise to be kept, several difficult limitations must be overcome, including the inseparable cations from the solvent that reside in the framework pore.

Keywords: ionothermal synthesis, metal organic frameworks, imidazolium-based ionic liquids, chemical trend analysis, structure simplification

1. Introduction

Three things are necessary to consider in the preparation of metal organic frameworks (MOFs): the metal, organic ligand, and solvent. Often neglected is the influence exerted by the solvent on the eventual framework, unlike the metal and the ligand that the structure always constitutes of. Varying the key characteristics of the solvent, such as hydrophilicity, is often the deciding factor in the reaction yield and the nature of the final compound [1]. Until 2002, when Jin et al. first used ionic liquids to synthesise metal organic framework [2], the list of solvents in inorganic synthesis was limited to few organic solvents and water [3]. This new synthesis method received growing attention in the field of MOFs to open a new realm of novel structures and provocative findings regarding the very nature of nanoscale synthesis. One aspect of ionothermal synthesis that contributed to its attention must have been its simplicity; the overall process comprises no more than mixing the metal salt and the organic ligand with the ionic solvent and incubating at a high temperature for long enough time. Unfortunately, however, the growth seems to have ceded in the recent years as shown in **Figure 1**. Given its distinctive potentials, this chapter is dedicated to introduce the field and draw more efforts for the full realisation of what the methodology dare to have promised. Before we move to the discussion of ionothermal synthesis and its potentials, the chemistry of ionic liquids

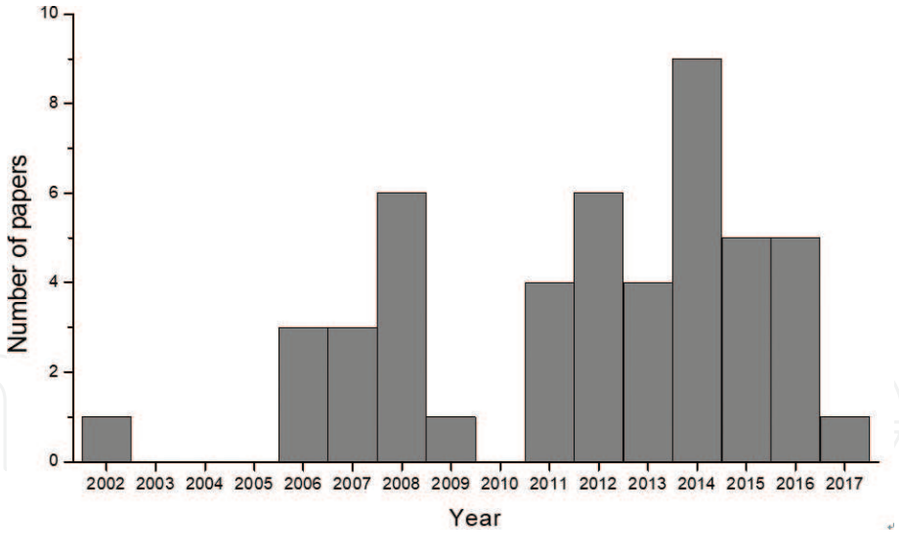

Figure 1.
Number of papers published annually under the topic of the ionothermal synthesis of MOFs since its first report.

must be first visited since it is this distinctive nature that lies behind all positive aspects, and limitations too, of ionothermal synthesis.

Ionic liquids are simply salts in the liquid state as opposed to the liquids typically used as solvents, [4] which are predominantly comprised of electrically neutral molecules. While most salts may be brought to their liquid states by heating, the term 'ionic liquids' is exclusively used for those that stay fluid around or below 100°C to distinguish them from the older phrase 'molten salts' [5]. One reason behind the attention that ionothermal methodology receives may be directly induced from the term 'ionic liquid' itself. The liquids are held by ionic interactions that far outcompetes the most intermolecular interactions in other solvents, including the renowned hydrogen bonds in water. Such strong interaction is responsible for their low vapour pressure [6], which could resolve the safety and environmental concerns associated with conventional organic solvents [5]. Such characteristics function as the exact same advantages in synthesis of MOFs. Nevertheless, the synthesis has greater potential in which the reaction environment can be finely tuned by modifying the solvent ions [7]. There are only several hundreds of molecular solvents, whereas a million binary combinations and a million of millions of ternary combinations possible for ionic liquids [5], hence their nickname 'designer solvent [8]'. Efforts in the field need to be focused not only on collecting outcomes from as many combinations as possible, but also, more importantly, on comprehending the laws of chemistry lying behind the trend observable in those data. This shall, as more than enough possible combinations await, ultimately enable designing the product for a given purpose, rather than vice versa.

This chapter will focus on showing the potentials of ionothermal synthesis by presenting a set of related syntheses in an organised manner. A series of such ionic liquids (RMI-X) may be prepared with 1-alkyl-3-methylimidazolium (RMI) and halide ions(X) [9]. This series of solvents exhibit finest tunability, in addition to their stability, with its variable length of alkyl side chain of the cation and the anion species variable along the halide column, which places them among the most extensively studied solvents for ionothermal synthesis of MOFs. To confirm their dominance in structure reports and the focus of our discussion on them, investigations have been made about the number of MOFs synthesised with several popular ionic liquids. The scope of our search—the list of cations and anions comprising the most common ionic liquids—has been illustrated in **Figure 2**. According to Cambridge Structural Database (CSD), it was shown that much of the reported MOFs is synthesised from

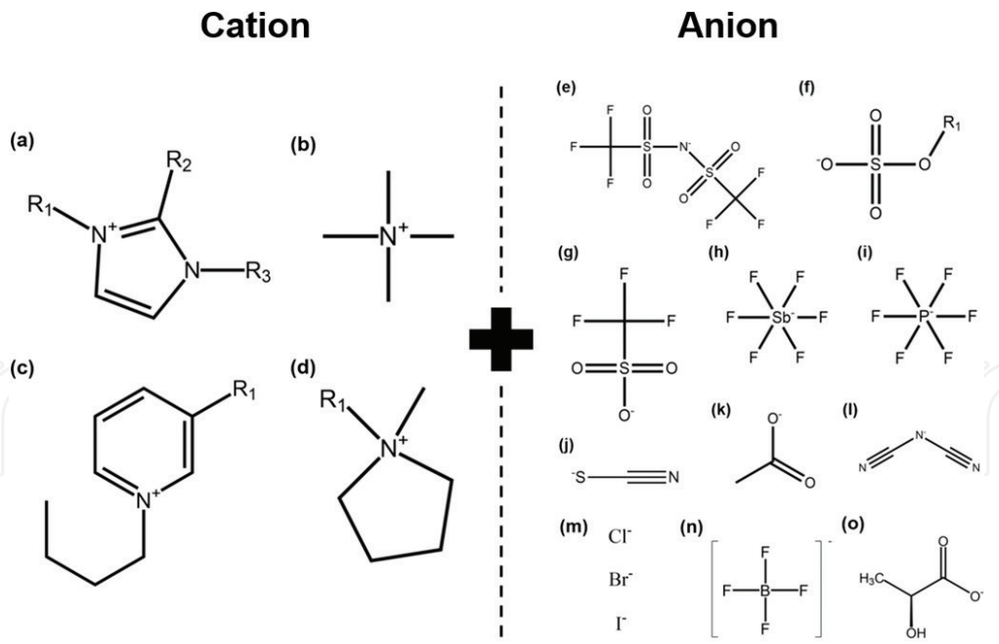

Figure 2.
Common cations and anions that composes an ionic liquid. Different combination of cations and anions results in various characteristics and gives rise to the diversity of topology and structure in synthesised MOFs. (a) Imidazolium (R_1 = methyl, ethyl, butyl; R_2 = hydrogen, methyl; R_3 = methyl, ethyl, propyl, butyl, pentyl, hexyl, octyl, benzyl, allyl, vinyl); (b) Ammonium; (c) Pyridinium (R_1 = hydrogen, methyl); (d) Pyrrolidinium (R_1 = ethyl, propyl, butyl, hexyl); (e) Bis((trifluoromethyl)sulfonyl)amide; (f) Alkyl sulphate (R_1 = methyl, ethyl); (g) Trifluoromethanesulfonate; (h) Hexafluorostibate(V); (i) Hexafluorophosphate(V); (j) Thiocyanate; (k) Acetate; (l) Bis(cyanide)amide; (m) Halide ion; (n) Tetrafluoroborate; (o) L-lactate.

ionic liquids that contains imidazolium and halide ions. There are no MOF crystal containing pyridium cation, and only few crystals synthesised from tetramethyl ammonium is reported as MOF. Synthesis using pyrrolidinium cation shows about 100 crystals, which corresponds to co-crystal form, showing that no crystal exhibits MOFs including pyrrolidinium cation. Extensiveness of data is the foundation of all successful discussions. With the extensiveness of RMI-X now taken for granted, structures synthesised from conditions with piecemeal differences, namely the length of the side chain of the cation, halide ions, and core metal atom of the structure were analysed to explore the effect on the final product arising from such variations.

2. Gradual difference in the solvent brings about gradual difference in the product

An important characteristic of ionothermal synthesis is that the characteristics of the solvents may be gradually varied and investigate the difference induced in the final product. While the solvent can be substituted with a complete different class of cations or anions to provide a completely reshaped environment, more minor changes can be made to the ions so that the change is gradual and quantifiable. Changing the length of the alkyl side chains attached to imidazolium cations, or changing the anions within the halide column to gradually change the size of the solvent ions is one example that will be mainly discussed in the chapter. This way, we may grasp a better understanding of the relation between the beginning and the end of this nanoscopic synthesis. Actually, organic solvents hold the exact same advantage, seeing that even the size variation of imidazolium cations is actually an organic one. However, in ionic liquids, this variation is expanded to a two-dimensional table for binary combinations, and possibly to even four-dimensional

construct for ternary combinations, which can provide more organised data is obvious. A better understanding of the nature is a foundation for a better utilisation of chemistry for many types of benefits. This section will guide you to the exploration that searches for new meaningful correlations in the sea of ionothermally prepared materials as the size of the solvent.

2.1 Correlation between the solvent and the product is often very simple

The correlation between the solvent and the product is perhaps the easiest to perceive in the system of frameworks synthesised with nickel and 1,3,5-benzenetricarboxylic acid(BTC). In **Table 1**, the structure shifts from the A-topology to the B-topology as we move down to the table and increase the cation size [1]. The shift occurs at smaller cations when we move right to the table to increase the anion size. It appears the size of the solvent, the cation and the anion considered together, is the key factor in determining the topology between A and B. From just this trend alone, it may be inferred that the B topology has a larger pore size, that is more empty space in the framework, than the A topology, which complies with the framework analyses by X-ray diffractions. There are certainly more reasons to this and we will come back to this later in the chapter, but for now, it is enough to just appreciate the simplicity of trend analysis.

The shift in the size of the ionic liquid exerted strong enough a pressure to give rise to two totally different topologies, but sometimes, the shift may be minor. In manganese-BTC system presented in **Table 2**, all three combinations in the [EMI] row gave rise to the exact same structure, α1 [10]. However, in the [PMI] column, only chloride and bromide gave rise to α2, and iodide to a slightly different α3. It is predicted that [EMI] cation is too small to induce a structure transition to occur in the row, but [PMI] is big enough to do so. Even though all the reported cases

$Ni(OAc)_2{\cdot}H_3BTC$	Cl	Br	I
[EMI]	A1	A1	A1
[PMI]	A2	A2	B1
[BMI]	A3	B2	B2
[PEMI]	B3	B3	B3

Structures sharing a topological identity were labelled under the same alphabet, while the numbers denote minor difference among them. Each labels denote, $[RMI]_2[Ni_3(BTC)_2(OAc)_2]$ (RMI = EMI for A1, PMI for A2, BMI for A3), $[RMI]_2[Ni_3(HBTC)_4(H_2O)_2]$ (RMI = BMI for B2, PEMI for B3). A1, A2, A3, B1, B2 reported in [1], and B3 in [7].

Table 1.
Organisation of structures in Nickel-BTC system on the length of the alkyl side chain of the cation and the halide anion.

$Mn(OAc)_2{\cdot}H_3BTC$	Cl	Br	I
[EMI]	α1	α2	α1
[PMI]	α2	α2	α3
[BMI]	—	—	—
[PEMI]	—	—	—

Each labels denote, α1-[EMI][Mn(BTC)], α2-[PMI][Mn(BTC)], α2-[PMI][Mn(BTC)]. Combinations that have not been reported were left blank. All entries were reported in [10].

Table 2.
*A table for the system of framework synthesised with manganese-BTC system arranged similarly to **Table 1**.*

in the system belong to the same topology class, but when the smaller differences were accounted, the table again shows a similar stair-shaped pattern that may be explained using the exact same argument.

$Cd(OAc)_2{\cdot}H_3BTC$	Cl	Br	I
[EMI]	a1 [12]	b1 [12, 13]	b1 [12]
[PMI]	b2 [12]	b2 [12]	b2 [12]
[BMI]	—	—	—

Each labels denote, a1-[EMI][Cd2(BTC)Cl2] for a1, [RMI][Cd(BTC)] (EMI for b1, PMI for b2). Combinations that have not been reported were left blank. Reference in literature to which the entries may be corresponded to has been indicated next to the entries in the table.

Table 3.
A table for the system of framework synthesised with cadmium-BTC system arranged similarly to ***Table 1****.*

M	Formula	Nuclear #	CCDC code	Void with cation*	Void without cation*
Co	$[EMI]_2[Co_3(BDC)_3Cl_2]$	Tri-nuclear	TACHUD [14]	0% 0 Å^3 /2088.3 Å^3	39.6% 827.3 Å^3 /2088.3 Å^3
	$[PMI]_2[Co_3(BDC)_3Cl_2]$	Tri-nuclear	TACJAL [14]	0% 0 Å^3 /2106.8 Å^3	39.8% 839.6 Å^3 /2106.8 Å^3
	$[BMI]_2[Co_3(BDC)_3Cl_2]$	Tri-nuclear	TACJEP [14]	0% 0 Å^3 /2082.1 Å^3	40.0% 832.7 Å^3 /2082.1 Å^3
	$[AMI]_2[Co_3(BDC)_3Cl_2]$	Tri-nuclear	TACJIT [14]	0% 0 Å^3 /2314.1 Å^3	46.8% 1083.9 Å^3 /2314.1 Å^3
	$[EMI]_2[Co_3(BDC)_3Br_2]$	Tri-nuclear	JOQXOE [15]	1.7% 35.2 Å^3 /2103.5 Å^3	38.9% 817.7 Å^3 /2103.5 Å^3
	$[PMI]_2[Co_3(BDC)_3Br_2]$	Tri-nuclear	JOQXUK [15]	0.6% 13.0 Å^3 /2123.4Å^3	40.0% 848.5 Å^3 /2123.4 Å^3
	$[BMI]_2[Co_3(BDC)_3Br_2]$	Tri-nuclear	JOQPUC [15]	0% 0 Å^3 /2172.6 Å^3	40.4% 877.1 Å^3 /2172.6 Å^3
	$[AMI]_2[Co_3(BDC)_4]$	Tri-nuclear	JOQQAJ [15]	17.0% 1001.9 Å^3 /5898.3 Å^3	52.2% 3081.8 Å^3 /5898.3 Å^3
	$[EMI]_2[Co_3(BDC)_3I_2]$	Tri-nuclear	TACJOZ [14]	1.4% 31.0 Å^3 /2184.2 Å^3	40.3% 879.5 Å^3 /2184.2 Å^3
	$[PMI]_2[Co_3(BDC)_3I_2]$	Tri-nuclear	TACJUF [14]	0.9% 20.9 Å^3 /2201.7Å^3	41.5% 914.8 Å^3 /2201.7 Å^3
	$[BMI]_2[Co_3(BDC)_3I_2]$	Tri-nuclear	TACKAM [14]	0% 0 Å^3 /2267.4Å^3	39.7% 901.0 Å^3 /2267.4 Å^3
	$[AMI]_2[Co_3(BDC)_3I_2]$	Tri-nuclear	TACKEQ [14]	0% 0 Å^3 /2275.1 Å^3	44.7% 1017.9 Å^3 /2275.1 Å^3

M	Formula	Nuclear #	CCDC code	Void with cation*	Void without cation*
Zn	$[EMI]_2[Zn_3(BDC)_3Cl_2]$	Tri-nuclear	SIVQEV [16]	0% 0 $Å^3$ /2085.2 $Å^3$	39.6% 826.7 $Å^3$ /2085.2 $Å^3$
	$[PMI]_2[Zn_3(BDC)_3Cl_2]$	Tri-nuclear	QUGVAR [17]	0% 0 $Å^3$ /2097.0$Å^3$	39.7% 833.2 $Å^3$ /2097.0 $Å^3$
	$Zn(BDC)(H_2O)$	Poly-nuclear	IFABIA03 [17]	0% 0 $Å^3$ /826.8 $Å^3$	0% 0 $Å^3$ /826.8$Å^3$
	$[BMI]_2[Zn_3(BDC)_3Cl_2]$	Tri-nuclear	SIVCAD [16]	0% 0 $Å^3$ /2167.9 $Å^3$	41.7% 903.4 $Å^3$ /2167.9 $Å^3$
	$[EMI]_2[Zn_3(BDC)_3Br_2]$	Tri-nuclear	QUGVIZ [17]	0.8% 16.5 $Å^3$ /2115.0 $Å^3$	39.9% 844.0 $Å^3$ /2115.0 $Å^3$
	$[PMI]_2[Zn_3(BDC)_3Br_2]$	Tri-nuclear	QUGVOF [17]	0.6% 11.9 $Å^3$ /2139.4 $Å^3$	40.6% 868.6 $Å^3$ /2139.4 $Å^3$
	$[BMI]_2[Zn_3(BDC)_3Br_2]$	Tri-nuclear	QUGVUL [17]	0% 0 $Å^3$ /2189.2 $Å^3$	42.1% 921.1 $Å^3$ /2189.2 $Å^3$
	$[EMI]_2[Zn_3(BDC)_3I_2]$	Tri-nuclear	QUGWEW [17]	0.6% 12.1 $Å^3$ /2169.2 $Å^3$	40.0% 868.7 $Å^3$ /2169.2 $Å^3$
	$[PMI]_2[Zn_3(BDC)_3I_2]$	Tri-nuclear	QUGWIA [17]	0% 0 $Å^3$ /2182.0 $Å^3$	40.4% 882.6 $Å^3$ /2182.0 $Å^3$
	$[BMI]_2[Zn_3(BDC)_3I_2]$	Tri-nuclear	QUGWOG [17]	0% 0 $Å^3$ /2253.3 $Å^3$	39.7% 894.2 $Å^3$ /2253.3 $Å^3$
	$[AMI]_2[Zn_3(BDC)_3I_2]$	Tri-nuclear	QUGWUM [17]	0% 0 $Å^3$ /2293.1 $Å^3$	40.7% 933.1 $Å^3$ /2293.1 $Å^3$
Eu	$[EMI][Eu_2(BDC)_3Cl]$	Di-nuclear	IXISOZ02 [18]	0%, 0 $Å^3$ /2339.26 $Å^3$	30.5% 714.34 $Å^3$ /2339.3 $Å^3$
	$[PMI][Eu_2(BDC)_3Cl]$	Di-nuclear	IXITOA02 [18]	4.6% 157.3 $Å^3$ /3429.0 $Å^3$	30.8% 1055.9 $Å^3$ /3429.0 $Å^3$
	$[BMI][Eu_2(BDC)_3Cl]$	Di-nuclear	IXITIU02 [18]	0.2% 14.7 $Å^3$ /6850.9 $Å^3$	29.8% 2038.9 $Å^3$ /6850.9 $Å^3$
	$[EMI][Eu_2(BDC)_3(H_2BDC)Cl_2]$	Poly-nuclear	YIXFOC03 [19]	0% 0 $Å^3$ /3153.1$Å^3$	21.4% 673.7 $Å^3$ /3153.1 $Å^3$
	$Eu(BDC)(CO_2)$	Poly-nuclear	LARYEK03 [20]	0% 0 $Å^3$ /929.6 $Å^3$	0% 0 $Å^3$ /929.6 $Å^3$
	$Eu_3(BDC)_4Cl(H_2O)_6$	Poly-nuclear Mono-nuclear	IXITEQ02 [18]	0% 0 $Å^3$ /3605.0 $Å^3$	0% 0 $Å^3$ /3605.0 $Å^3$
	$Eu(BDC)Cl(H_2O)$	Poly-nuclear	IXISIT02 [18]	0% 0 $Å^3$ /975.0 $Å^3$	0% 0 $Å^3$ /975.0 $Å^3$

M	Formula	Nuclear #	CCDC code	Void with cation*	Void without cation*
In	$[EMI]_2[In_2(BDC)_3Br_2]$	Mono-nuclear	SABJOX [21]	0% 0 Å^3 /2017.0 Å^3	36.0% 725.1 Å^3 /2017.0 Å^3
	$[PMI]_2[In_2(BDC)_3Br_2]$	Mono-nuclear	SABJIR [21]	0% 0 Å^3 /2073.5 Å^3	36.0% 746.0 Å^3 /2073.5 Å^3
Dy	$[EMI][Dy_3(BDC)_5]$	Poly-nuclear	RINTUF [22]	2.8% 134.8 Å^3 /4840.8 Å^3	21.2% 1027.3 Å^3 /4840.8 Å^3
Tb	$[EMI][Tb_2(\mu_2\text{-}Cl)(BDC)_3]$	Poly-nuclear	YIXFUI [19]	19.7% 620.8 Å^3 /3152.5 Å^3	19.7% 620.8 Å^3 /3152.5 Å^3
Sm	$[EMI]_2[Sm_2(BDC)_3(H_2\text{-}BDC)Cl_2]$	Di-nuclear	YIXFIW [19]	0% 0 Å^3 /2333.3 Å^3	30.4% 709.1 Å^3 /2333.3 Å^3
Cd	$[BMI]_2[Cd(BDC)_3Br_2]$	Tri-nuclear	QETDAV [23]	0% 0 Å^3 /2353.8 Å^3	40.4% 950.6 Å^3 /2353.8 Å^3
Cu	$[EEIM][NaCu(BDC)_2]$	Poly-nuclear	VOBRUB [24]	0% 0 Å^3 /2200.5 Å^3	31.3% 688.2 Å^3 /2200.5 Å^3

**Probe radius of 1.2 Å and grid spacing of 0.7 Å was taken for the calculation using the contact surface.*

Table 4.
Chemical formulas of structures arising from imidazolium-based MOFs with BDC are presented with their nuclear type, CCDC reference code, void volume with and without the residing cation, and the reference in literature that each structure was reported.

2.2 Ionic liquids function both as a solvent and template

Similar trends may also be found in other metals, despite less well-pronounced than nickel. The similarity may not be noticed at first glance, but it is the same stair-shaped pattern to nickel system. The topology shift just takes place with smaller ionic species. Again, increase in size of the ionic solvent has changed the preferred topology to another class with a larger pore volume to incorporate the ions. As some readers might have noticed by now, here is a good point to introduce another interesting aspect of ionothermal synthesis; ionic liquids function not only as solvents, but also as a template that physically exerts a pressure to determine the final topology by residing in the framework [11] (**Table 3**).

2.3 Many reported syntheses are yet to fit into an organised system

In theory, many choices of organic linkers available in the field of chemistry may add to the large number of ionic combinations to create nearly infinite possible cases, but it takes time for a theory to become reality. While many valuable efforts are being made to contribute, those with 1,3,5-bezenetricarboxylic acid(BTC) and 1,4-benzenedicarboxylic acid(BDC) have done its part particularly extensively and the reported structures were organised in **Tables 4** and **5**. **Tables 4** and **5** are great to appreciate the variety of ionothermally prepared MOFs, plus for searching purposes, but give hardly any information on the chemical reaction that brought about the structures. In order to get a closer grasp on how ionothermal synthesis produced this variety, they must be organised into systems of related syntheses. However, many cases in both tables are rather discrete. Efforts need to be made, starting from what have been reported, to expand the literature by applying the ionic liquid to gradual variations.

M	Formula	Nuclear #	CCDC	Void with cation*	Void without cation*
Ni	$[EMI]_2[Ni_3(BTC)_2(OAc)_2]$	Tri-nuclear	VEMSUC [25]	0% 0 Å^3 /3704 Å^3	36.5% 1350.8 Å^3 /3704 Å^3
	$[PMI]_2[Ni_3(BTC)_2(OAc)_2]$	Tri-nuclear	XUJPIC [1]	0.9% 26.4 Å^3 /2780.4 Å^3	38.7% 1076.8 Å^3 /2780.4 Å^3
	$[BMI]_2[Ni_3(BTC)_3(OAc)_2]$	Tri-nuclear	XUJPOI [1]	0% 0 Å^3 /3802.9 Å^3	0% 0 Å^3 /3802.9 Å^3
	$[PMI]_2[Ni_3(HBTC)_4(H_2O)]$	Tri-nuclear	VEMSUC01 [1]	0% 0 Å^3 /3712.3 Å^3	36.7% 1363.0 Å^3 /3712.3 Å^3
	$[BMI]_2[Ni_3(HBTC)_4(H_2O)]$	Tri-nuclear	XUJQAV [1]	0% 0 Å^3 /3806.2 Å^3	0% 0 Å^3 /3806.2 Å^3
	$[BMI]_2[Ni(HBTC)_2(H_2O)_2]$	Tri-nuclear	NUNNUH [26]	3.4% 132.7 Å^3 /3944.7 Å^3	53.6% 2113.7 Å^3 /3944.7 Å^3
	$[BMI]_2[Ni(HBTC)_2(H_2O)_2]$ chiral	Tri-nuclear	NUNPAP [26]	3.2% 124.9 Å^3 /3953.2 Å^3	53.6% 2120.3 Å^3 /3953.2 Å^3
	$[AMI][Ni_3(BTC)_2(OAc)(MI)_3]$	Mono-nuclear Di-nuclear	EGOYUV [27]	0% 0 Å^3 /4592.0 Å^3	22.4% 1029.7 Å^3 /4592.0 Å^3
Co	$[EMI][Co_2(HBTC)_2(4,4'\text{-}bpy)_3]Br$	Di-nuclear	YODYUM [28]	0% 0Å^3 /5060.8 Å^3	13.6% 688.9 Å^3 /5060.8 Å^3
	$[EMI][Co(HBTC)(4,4'\text{-}bpy)_2]$ (4,4′-bpy)Br	Mono-nuclear	YODZAT** [28]	0% 0 Å^3 /4290.3 Å^3	17.8% 762.0 Å^3 /4290.3 Å^3
	[EMI][Co(BTC)(H-Im)]	Mono-nuclear	YODZEX [28]	0% 0 Å^3 /933.9 Å^3	30. 1% 280.63 Å^3 /933.9 Å^3
	$[EMI]_2[Co(BTC)_2(H_2TED)]$	Mono-nuclear	YODZIB [28]	0% 0 Å^3 /7246.2 Å^3	30.7% 2221.6 Å^3 /7246.2 Å^3
	$[EMI]_2[Co_3(BTC)_2(OAc)_2]$	Tri-nuclear	VEMTAJ [25]	38.6% 1466.9 Å^3 /3797.9 Å^3	38.6% 1466.9 Å^3 /3797.9 Å^3
	[EMI][Co(BTC)]	Di-nuclear	CIPLIX [29]	0% 0 Å^3 /3018.2 Å^3	26.0% 784.2 Å^3 /3018.2 Å^3
	[EMI] $[Co_2(BTC)_4H_7(2,2'\text{-}bpy)_2]$	Mono-nuclear	CIPLOD [29]	16.1% 483.0 Å^3 /3002.0 Å^3	16.1% 483.0 Å^3 /3002.0 Å^3
	$[PMI]_2[Co_2(BTC)_2(H_2O)_2]$	Di-nuclear	XAPSIS [30]	0% 0 Å^3 /1850.4 Å^3	51.1% 945.9 Å^3 /1850.4 Å^3
	$[BMI]_2[Co_2(BTC)_2(H_2O)_2]$	Di-nuclear	[31]	0% 0 Å^3 /1840.5 Å^3	51.8% 952.94 Å^3 /1840.5 Å^3
	$[EMI]_2[In_2Co(OH)_2(BTC)_2Br_2]$	Tri-nuclear (In + Co)	VUVZAP [32]	0% 0 Å^3 /1884.5 Å^3	36.6% 690.4 Å^3 /1884.5 Å^3

M	Formula	Nuclear #	CCDC	Void with cation*	Void without cation*
Zn	[BMI][Zn_2(BTC)(OH)I]	Tetra-nuclear	VIWZOR [33]	4.7% 106.8 Å^3 /2260.6 Å^3	49.4% 1117.8 Å^3 /2260.6 Å^3
	[BMI]$_2$[Zn_4(BTC)$_3$(OH)(H_2O)$_3$]	Tri-nuclear	MIQLEE [34]	4.8% 228.0 Å^3 /4739.5 Å^3	38.4% 1819.6 Å^3 /4739.5 Å^3
	[AMI][Zn_2(BTC)(OH)Br]	Tetra-nuclear	MIQLII [34]	0% 0 Å^3 /2229.3 Å^3	51.0% 1137.0 Å^3 /2229.3 Å^3
	[EMI][Zn(BTC)]	Di-nuclear	MIQKUT [34]	0% 0 Å^3 /3077.8 Å^3	38.2% 1175.6 Å^3 /3077.8 Å^3
	[PMI][Zn(BTC)]	Mono-nuclear	MIQLAA [34]	0% 0 Å^3 /3353.5 Å^3	43.9% 1472.9 Å^3 /3353.5 Å^3
	[Zn_3(BTC)$_2$(H_2O)$_2$]·2H_2O	Poly-nuclear	MISRUC [34]	0% 0 Å^3 /1985.1 Å^3	0% 0 Å^3 /1985.1 Å^3
	[Zn_4(BTC)$_2$(μ_4-O)(H_2O)$_2$]	Tetra-nuclear	XOHLEM [35]	37.7% 1293.1 Å^3 /3431.7 Å^3	37.7% 1293.1 Å^3 /3431.7 Å^3
	[BMI][Zn(BTC)]	Di-nuclear	FUTZEB [36]	0% 0 Å^3 /1678.8 Å^3	46.8% 786.5 Å^3 /1678.8 Å^3
Cd	[EMI][Cd_2(BTC)Cl_2]	Poly-nuclear	SIZGEO [12]	0% 0 Å^3 /924.3 Å^3	34.0% 314.7 Å^3 /924.3 Å^3
	[EMI][Cd(BTC)]	Di-nuclear	NEHMET [13]	0% 0 Å^3 /3181.9 Å^3	43.4% 1381.4 Å^3 /3181.9 Å^3
	[PMI][Cd(BTC)]	Di-nuclear	SIZGIS [12]	0% 0 Å^3 /3296.9 Å^3	43.2% 1425.3 Å^3 /3296.9 Å^3
Mn	[EMI][Mn(BTC)]	Di-nuclear	WEYQAU [10]	0% 0 Å^3 /3051.7 Å^3	38.7% 1181.6 Å^3 /3051.7 Å^3
	[PMI][Mn(BTC)]	Di-nuclear	WEYQEY [10]	0% 0 Å^3 /3229.3 Å^3	42.8% 1382.5 Å^3 /3229.3 Å^3
	[PMI][Mn(BTC)]	Di-nuclear	WEYPUN [10]	0% 0 Å^3 /3172.0 Å^3	45.8% 1451.3 Å^3 /3172.0 Å^3

**Calculation was done with the same setting. Calculation for the entry 'void without cations' has been conducted by removing only the cations from the channel.*
***In the entry with reference code YODZAT, not only ionic cations but also 4,4'-bpy ligands were found in the channel.*

Table 5.
Structures arising from imidazolium-based MOFs with BTC presented in a similar manner to ***Table 1****.*

3. The correlation between the reaction solvent and the product

In the previous section, we have explored through the chemical trend observable in nickel, manganese, and cadmium-BTC systems. Some basic explanations have been provided by relating the size of the ionic species to the pore size

of each structure. However, many questions still remain to be answered. For example, why does the topology shift has to occur right there, not anywhere else? If even larger cations were used, will the topology remain unchanged or will a new one appear? In order to answer this question, we have to get a deeper knowledge about the structures and the ions of the solvent. Qualitative analyses were simple, but it becomes necessary to add numbers to our logics to advance further.

3.1 Trends to predict future outcomes

In the nickel-BTC system we first examined, increasing the cation size caused the topology to shift from the more condensed A-class to the B-class with a larger cavity volume. In **Table 1**, data have been provided from [EMI] to [PEMI] only. Suppose we are interested in the results for a new [HMI] column; the cation alkyl side chain increased by a carbon. The simplest way to predict the outcome is to analyse the cavity of the B-class topology and test if it is capable of housing the elongated [HMI] cations. In addition, taking a deeper look into the A-class topology might also strengthen our previous reasoning.

In the A-class topology, we can see that the cavities are not so well connected with each other [1, 7]. On the other hand, the B-class topology has cavities connected to their neighbours to create a linear channel-shaped pore as illustrated in **Figure 3**. The maximum length of the cation that can fit into the A-class topology is limited, but it is not so in the B-class topology. After looking at how the structures actually look like, we can now more confidently say that elongating the cation by a carbon is unlikely to exert enough pressure on the framework to give rise to a new topology.

The next step is to test whether the predictions are correct. When a completely new material is synthesised and its structure is to be determined, advanced tools like single-crystal X-ray diffractions must be used to resolve all positions of the atoms in the unit cell. However, when we have a reference material with a known structure, simpler techniques like powder X-ray diffractions (PXRD) are enough to tell whether the new material has the same structure to the reference. Therefore, the common step is to obtain the PXRD graph and compare it to the graph of some suspected structures. It is only when the new graph is different enough, the new material is subjected to complete structure analysis. Since our expectation was that the entries for the [HMI] column will have the same topology to the [BMI] column, we took the PXRD data for two and compared as in **Figure 4**. To assure the topological identity, several different combinations have been selected. All major peaks occur at the same angles, and our prediction by extrapolation has been proven valid [7]. We have now seen that correlations are valuable in that they may be used to predict future outcomes. This is the moment where prediction is no more but only an extrapolation.

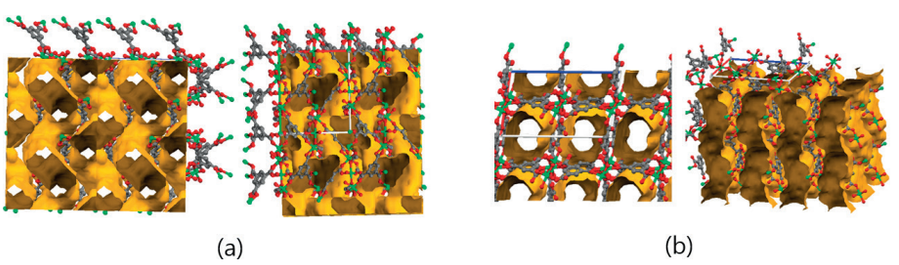

Figure 3.
Diagrams depicting the pores of (a) the A-class topology and (b) the B-class topology at Ni-BTC system. The linear shaped channels of the B-class topology become evident [7].

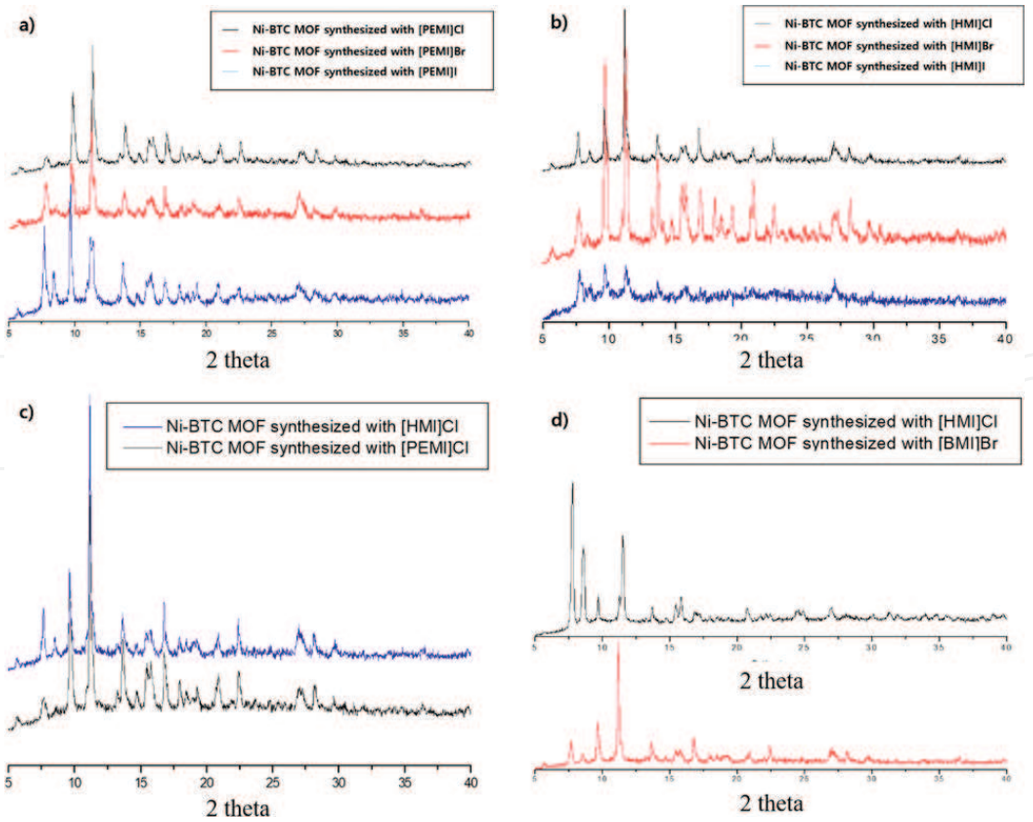

Figure 4.
PXRD data presented in pairs or triplets to illustrate the similarity and difference of the topologies occurring in the Ni-BTC system. (a) Structures synthesised from [PEMI]Cl, [PEMI]Br, and [PEMI]I show that all three in the [PEMI] row belong to the same topology group. (b) Three structures from [HMI] row show that they belong to the same topology group similarly to (a). (c) Two structures from the Cl column show that the topology groups of [HMI] row and [PEMI] row are identical. (d) The structure synthesised from [HMI]Cl is compared to that from [BMI]Br and shows that each two belong to the same class. The magnitude may be different, but the positions of the main peaks coincide [7].

3.2 The effect of the final framework on the solvent properties

The trend extrapolation introduced above was a success, but by no means is a guarantee that similar arguments will always hold true. All scientific explanations are based on reductive models where many details in reality must have been missed. However, discussions until now have only focused on how the variance in solvent properties, namely size, give rise to another variance in the product framework, but never vice versa. Chemistry is a study of interactions, and the term 'interactions' imply that there may always be bidirectional influence. It surely is the solvent that was in the reaction system first and then frameworks were built on top of the influence of the solvent, and thus, its influence on the product is more pronounced and also more important. However, the ionic species residing in different structures are in fact different even if they were in the same bottle before being deployed to the reaction. We would now like to guide your attention to an interesting system where the framework exerts a strong pressure to the cation to alter its shape. In such cases, extrapolations may not give accurate results.

Table 6 shows three reported entries in the not-so-extensively-studied cobalt-BTC system. Nevertheless, simplicity is not to be confused with incompleteness. While it may be true that the entire trend may not be fully described, deeper analysis may follow in a more complete manner for the part that has been, or at least it reduces the burden to describe so many entries in full details.

The bromide column is never an exception to the systems we have been through. The α-class topology has pore volume smaller than the β-class, and it is

$Co(OAc)_2{\cdot}H_3BTC$	Cl	Br	I
[EMI]	—	α1 [25]	—
[PMI]	—	β1 [30]	—
[BMI]	—	β2 [31]	—

Each labels denote, α1-$[EMI]_2[Co_3(BTC)_2(OAc)_2]$, β1- $[PMI]_2[Co_2(BTC)_2(H_2O)_2]$, and β2 -$[BMI]_2[Co_2(BTC)_2(H_2O)_2]$. Combinations that have not been reported were left blank.

Table 6.
A table for the system of framework synthesised with cadmium-BTC system arranged similarly to ***Table 1****.*

the increase in the cation size that caused it. However, a question that never has been addressed in previous systems was, is the difference between [EMI] to [PMI] the same as that between [PMI] and [BMI]? In other words, they are gradual, but are they in scale? They both differ by a carbon, and carbon–carbon bond length is nearly universally conserved. It seems they should differ only by an iota, if they were even different after all.

The *in situ* conformations of the guest cations were taken and subjected to computational analysis [31]. The difference in volume between [EMI] and [PMI] was calculated to be 21.8 $Å^3$, which is significantly larger than 14.9 $Å^3$, the difference between [PMI] and [BMI]. It is apparent that this difference arose from the bent conformation of the butyl chain of [BMI] cation; the distance between the terminal carbon to the first carbon in the chain was 2.918°A in compound β2, exceeding 2.567°A of compound β1 only by a small difference. The carbon–carbon bond is free to rotate about each other, but the β-class framework is stable enough to fix the conformation severely bent as they appear; a remarkable example of the framework influencing the property of the solvent. Moreover, just because it appears as the same one step on the table does not mean the actual size difference between the ionic species is the same.

Even though β1 and β2 structures belong to the same topology class, they may have minor differences like the ones described in the manganese system. Even by a small bit, [BMI] is still larger than [PMI] and is expected to exert pressure on the framework towards retaining a larger void volume. However, this straightforward prediction is actually far from the truth. The β-topology framework is so rigid that the void volume and the framework volume stay nearly unchanged for [PMI] and [BMI].

It also deserves some attention that the β-topology occurs very rare in other metal systems, suggesting that it is not so chemically favoured in many other environments [31]. While the rigidity of the framework can also be viewed as how favoured it is over other possible outcomes, it is interesting that this rare topology is so strongly preferred in the system and in cobalt system only. Also, attempts to synthesise crystalline frameworks with [PEMI]Br and [HMI]Br in the system all failed but only acquired amorphous solids. This further supports the absence of any other stable framework possible in the cobalt system. Additional studies must follow to provide explanations for the strikingly different preference of framework in the cobalt system.

4. Reducing topologies can easily deliver deep insights into the structures

The structural details of nanoscopic frameworks are often difficult to perceive. Some basic discussion may be made even with the structures completely ignored, but we already have seen many limitations to that. Understanding the structure is necessary to provide more thorough explanations for the chemical trends appearing

in the organised systems of ionothermally prepared MOFs, including many unusual cases unexplainable by simple intuition. Just like organic chemistry cannot be approached without molecular formulas, inorganic chemistry cannot be explained without framework structures. We would like to dedicate this chapter to suggest a method to break down the complications of nanoscopic structures to see the forest beyond the trees, and lastly, tour around that forest.

4.1 Metals atoms tend to exist in clusters

In order to bring down the structures to simpler diagrams, the patterns, or segments of atoms, that occur frequently throughout the framework must be well noticed. After taken the knowledge of the building blocks, we will look into a representative building to see how the blocks are assembled to a building. It is obvious that the organic linker will stay as it is used before the reaction in most structures, as it is very difficult for the benzene ring to disassemble in our BTC example. One thing, however, may fluctuate greatly from structure to structure: the coordination mode. Often there are many atoms, or sites, that are capable of coordinating to metal atoms, but almost always, not all of them do. It is very difficult to predict which coordination mode the ligand will take, since even under the same topology, the ligands are found to take structures with many different coordination modes [1, 30, 31]. Attempts have been made to collectively study coordination modes [34], but for successful discovery of any laws governing them, acquisition of more data is necessary.

In collaboration with the coordination modes, though it is difficult to distinguish causation from correlation at this level, the reaction environment determines the shape in which the metal atoms exist in the framework. From **Tables 4**, **5** and **7**, it has been shown the nuclear types the metal atoms take in the framework, but the concept has never been visited yet. This 'nucleus' is a small collection of metal atoms and atoms from the organic ligand coordinating to them and is more commonly called 'metal clusters' because many metal atoms are found together in most structures. These metal clusters are one of the most important character to determine the topology of MOFs, and the frameworks are named as binuclear, trinuclear, etc. according to the number metal atoms present in the metal cluster. If small variations within the same topology are ignored, the framework can be viewed as a collection of simple connections between the unvarying organic ligand and the metal clusters, just like vertices and edges of a mathematical 3D figure.

The simplification illustrated in **Figure 5** exemplifies the power of reduction in brining different structures together. Although it could have been inferred from the same molecular formulas, a great number of structures introduced in **Tables 4**, **5** and **7** actually have the exact same framework.

4.2 Structure explains the popularity of [RMI][metal(BTC)] topology

Some of the most commonly occurring structures need attention, not only because they will be frequently met in trials of novel conditions, but also they will provide a valuable starting point in relating to other structures occurring in the same system to understand the correlations like the ones we have visited.

The topology [RMI][Metal(BTC)] occurs in most metal systems that have been reported and in the highest frequency. With this topology as an example, we will show how a complex structure may be simplified. This way, details unnecessary for understanding of the topology can be ignored and attention may be more easily focused on the topology itself. The characteristics that may vary within the topology without changing it include coordination modes, bond angle, and bond in certain ranges.

M	Formula	Nuclear #	CCDC code	Void with cation*	Void without cation*
Co	[EMI][Co(1,4-ndc)Br]	Di-nuclear	AHIYIB [37]	0% 0 Å^3 /1739.88 Å^3	37.8% 658.13 Å^3 /1739.88 Å^3
	$[PMI]_2[Co_7(1,4\text{-}ndc)_6(OH)_4]$	Hepta-nuclear	AHIYOH [37]	0% 0 Å^3 /8376.27 Å^3	23.4% 1958.42 Å^3 /8376.27 Å^3
	$[BMI]_2[Co_6(1,4\text{-}ndc)_6(OH)_2]$	Hexa-nuclear	AHIYUN [37]	0% 0 Å^3 /7998.16 Å^3	21.5% 1717.36 Å^3 /7998.16 Å^3
	$[AMI]_4[Co_4Na_5(1,4\text{-}ndc)_8Br]$	Tetra-nuclear	AHIZAU [37]	0% 0 Å^3 /6065.78 Å^3	31.3% 1897.74 Å^3 /6065.78 Å^3
Eu	$[EMI][Eu(1,4\text{-}ndc)(ox)_{0.5}Br]$	Poly-nuclear	EMUTUD [38]	0% 0 Å^3 /2033.18 Å^3	34.8% 708.05 Å^3 /2033.18 Å^3
	$[HMI][Eu_2Cl(1,4\text{-}ndc)_3]$	Poly-nuclear	MEGPIZ [39]	0% 0 Å^3 /4188.58 Å^3	26.0% 1086.94 Å^3 /4188.58 Å^3
Sm	$[HMI][Sm_2Cl(1,4\text{-}ndc)_3]$	Poly-nuclear	MEGPEV [39]	0% 0 Å^3 /4203.36 Å^3	25.8% 1086.30 Å^3 /4203.36 Å^3
	$[EMI][Sm(1,4\text{-}ndc)(ox)_{0.5}Br]$	Poly-nuclear	EMUVAL [38]	0% 0 Å^3 /2032.62 Å^3	34.9% 709.04 Å^3 /2032.62 Å^3
Mg	$[AMI]_2[Mg_3(1,4\text{-}ndc)_4(MeIm)_2(H_2O)_2]\cdot H_2O$	Tri-nuclear	EXUYEC [40]	0% 0 Å^3 /3424.65 Å^3	24.7% 845.14 Å^3 /3424.65 Å^3
	$[BMI]_2[Mg_6(1,4\text{-}ndc)_5(H_2NDC)_2(HCOO)_2]$	Hexa-nuclear	NUKBOM [41]**	0% 0 Å^3 /4700.01 Å^3	0% 0 Å^3 /4700.01 Å^3
Zn	$[EMI]_2[Zn_7(\mu_4\text{-}O)_2(1,4\text{-}ndc)_6]$	Hepta-nuclear	QATLEE [42]	0% 0 Å^3 /8044.7 Å^3	23.2% 1864.05 Å^3 /8044.7 Å^3
Ni	$[Ni_3(1,4\text{-}ndc)_4(Mim\text{-}C3Im)_2(H_2O)_2]$	Di-nuclear	TOLMOY [43]	0% 0 Å^3 /1704.13 Å^3	36.5% 622.27 Å^3 /1704.13 Å^3
	$[Ni_3(1,4\text{-}ndc)_4(Mim\text{-}C4Im)_2(H_2O)_2]$	Di-nuclear	TOLMUE [43]	0% 0 Å^3 /1721.79 Å^3	37.3% 642.55 Å^3 /1721.79 Å^3
	$[Ni_3(1,4\text{-}ndc)_4(Mim\text{-}C5Im)_2(H_2O)_2]$	Tri-nuclear	TOLNAL [43]**	0% 0 Å^3 /3276.26 Å^3	0% 0 Å^3 /3276.26 Å^3
	$[Ni_3(1,4\text{-}ndc)_4(Mim\text{-}C6Im)_2(H_2O)_2]$	Tri-nuclear	TOLNEP [43]**	0% 0 Å^3 /3387.26 Å^3	0% 0 Å^3 /3387.26 Å^3
Cd	[EMI][CdBr(1,4-ndc)]	Di-nuclear	UYUPUA [44]	0% 0 Å^3 /1814.56 Å^3	38.4% 697.55 Å^3 /1814.56 Å^3
Sr	$[EMI][Sr_{10}(1,4\text{-}ndc)_{10}Br_4]$	Poly-nuclear	VUXGOM [45]	0.2% 17.02 Å^3 /6950.81 Å^3	18.4% 1279.20 Å^3 /6950.81 Å^3

M	Formula	Nuclear #	CCDC code	Void with cation*	Void without cation*
Na, Cu	[EMI][NaCu(1,4-ndc)$_2$]	Poly-nuclear	WIKZAT [44]	0.6% 16.45 Å^3 /2729.18 Å^3	25.7% 700.27 Å^3 /2729.18 Å^3
La	[HMI][La$_2$Cl(1,4-ndc)$_3$]	Poly-nuclear	MEGNIX [39]	0% 0 Å^3 /4328.43 Å^3	26.6% 1150.84 Å^3 /4328.43 Å^3
Ce	[HMI][Ce$_2$Cl(1,4-ndc)$_3$]	Poly-nuclear	MEGNOD [39]	0% 0 Å^3 /4296.06 Å^3	26.6% 1142.24 Å^3 /4296.06 Å^3
Pr	[HMI][Pr$_2$Cl(1,4-ndc)$_3$]	Poly-nuclear	MEGNUJ [39]	0% 0 Å^3 /4262.42 Å^3	26.3% 1122.11 Å^3 /4262.42 Å^3
Nd	[HMI][Nd$_2$Cl(1,4-ndc)$_3$]	Poly-nuclear	MEGPAR [39]	0% 0 Å^3 /4241.32 Å^3	26.4% 1121.26 Å^3 /4241.32 Å^3
Gd	[HMI][Gd$_2$Cl(1,4-ndc)$_3$]	Poly-nuclear	MEGPOF [39]	0% 0 Å^3 /4164.69 Å^3	25.7% 1069.98 Å^3 /4164.69 Å^3
Tb	[HMI][Tb$_2$Cl(1,4-ndc)$_3$]	Poly-nuclear	MEGPUL [39]	0% 0 Å^3 /4152.78 Å^3	25.7% 1066.29 Å^3 /4152.78 Å^3
Dy	[HMI][Dy$_2$Cl(1,4-ndc)$_3$]	Poly-nuclear	MEGQAS [39]	0% 0 Å^3 /4124.91 Å^3	25.5% 1052.86 Å^3 /4124.91 Å^3
Ho	[HMI][Ho$_2$Cl(1,4-ndc)$_3$]	Poly-nuclear	MEGQEW [39]	0% 0 Å^3 /4105.46 Å^3	25.4% 1044.15 Å^3 /4105.46 Å^3
Er	[HMI][Er$_2$Cl(1,4-ndc)$_3$]	Poly-nuclear	MEGQIA [39]	0% 0 Å^3 /4103.22 Å^3	25.4% 1040.46 Å^3 /4103.22 Å^3
Y	[HMI][Y$_2$Cl(1,4-ndc)$_3$]	Poly-nuclear	MEGQOG [39]	0% 0 Å^3 /4127.12 Å^3	25.5% 1052.17 Å^3 /4127.12 Å^3

Calculation was done with the same setting. In the entry with reference code NUKBOM, TOLNAL, and TOLNEP, the calculation for the void volume with the cation removed was not conducted since the cations were bound to the framework.

Table 7.
Structures arising from imidazolium-based MOFs with 1,4-naphthalene dicarboxylic acid (NDC) presented in a similar manner to ***Table 4****.*

The simplification above is itself beautiful but is meaningless if description of the topology is not accompanied. Description gives meaning to the structure and explanations for many of the observed phenomena.

Based on face-centred cubic lattice (FCC), the unit cell of [RMI][Metal(BTC)] is very compact. Its binuclear metal cluster occupies all the FCC sites, and BTC occupies the interstitial sites. There are eight BTC ligands, and the rest of the interstitial sites appear empty in **Figure 6**. These sites, however, are not actually empty. There are eight metal clusters and eight BTC ligands in the unit cell, but each metal cluster has double positive charge while BTC ligand has triple negative. The framework is negatively charged, as nearly every ionothermally synthesised framework is, and the charge balance is maintained by the guest cations occupying the rest of the

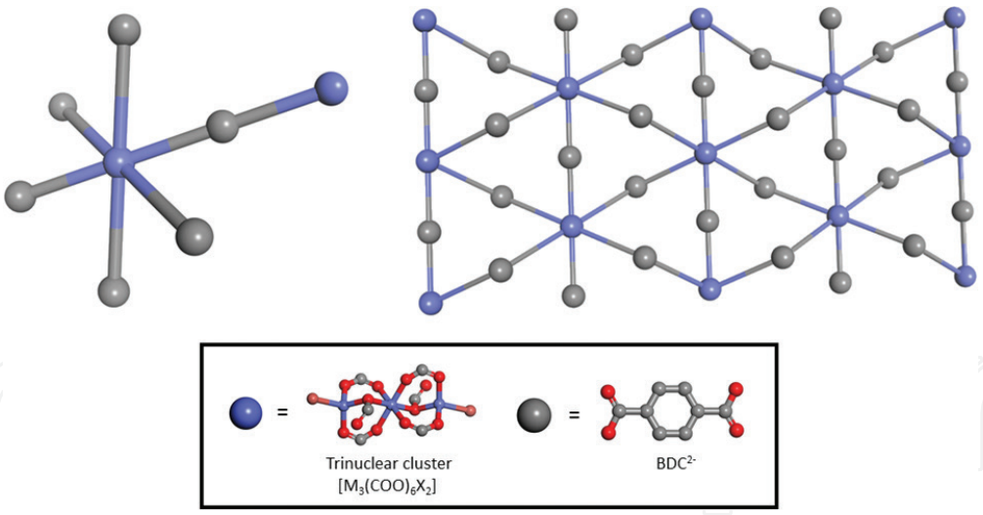

Figure 5.
The structure represents the (2,6)-connected 2D network. The list of entries that exhibit this particular structure is: $[EMI]_2[Co_3(BDC)_3X_2]$ (X = Cl, Br, I) (TACHUD for Cl; JOQXOE for Br; TACJOZ for I), $[PMI]_2[Co_3(BDC)_3X_2]$ (X = Cl, Br, I) (TACJAL for Cl; JOQXUK for Br; TACJUF for I), $[BMI]_2[Co_3(BDC)_3X_2]$ (X = Cl, Br, I) (TACJEP for Cl; JOQPUC for Br; TACKAM for I), $[PEMI]_2[Co_3(BDC)_3X_2]$ (X = Cl, I) (TACJIT for Cl; TACKEQ for I), $[EMI]_2[Zn_3(BDC)_3X_2]$ (X = Cl, Br, I) (SIVQEV for Cl; QUGVIZ for Br; QUGWEW for I), $[PMI]_2[Zn_3(BDC)_3X_2]$ (X = Cl, Br, I) (QUGVAR for Cl; QUGVOF for Br; QUGWIA for I), $[BMI]_2[Zn_3(BDC)_3X_2]$ (X = Cl, Br, I) (SIVCAD for Cl; QUGVUL for Br; QUGWOG for I), and $[PEMI]_2[Zn_3(BDC)_3X_2]$ (X = I) (QUGWUM for I).

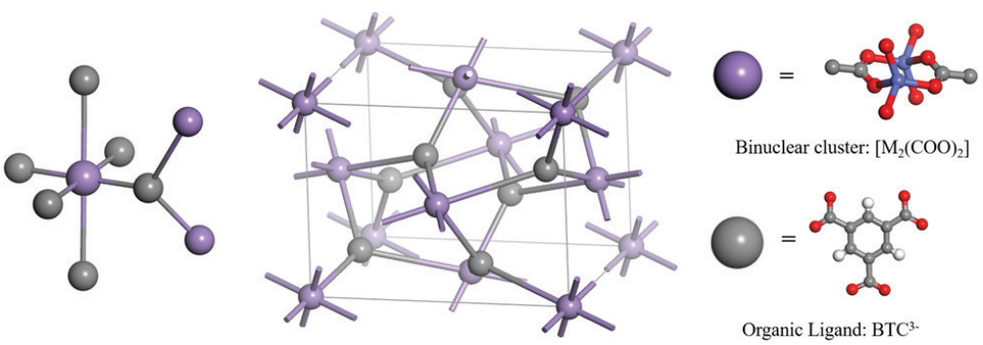

Figure 6.
The asymmetrical unit and the unit cell of [RMI][Metal(BTC)] topology with its binuclear cluster and organic ligand represented, respectively, by singular units.

interstitial sites. This allows no void for the structure and is thus stable. Nevertheless, the structure may not house longer cations regardless of how preferred it is over other possible options; it is just impossible. This complies with the observation from **Table 5** that the structure is very much preferred with [EMI], but only with [EMI] and the preference drops greatly as we move on to longer cations.

4.3 Seemingly different structures may belong to the same topology class

A large number of syntheses have been reported to the literature, but the number of novel topologies is much smaller. It will be very interesting to see so many structures that once appeared all different converging into one topology. In this example, a group of structures with a different formula and a different nuclear type will be merged with the [RMI][Metal(BTC)] class that has been described above.

Figure 7 depicts the [RMI][Metal(BTC)] structure. This same structure, however, is shared by $[EMI]_2[In_2Co(OH)_2(BTC)_2Br_2]$ structure that has a remarkably different molecular formula. The formula is the simplest tool to represent frameworks, but it can sometimes be misleading. **Figure 8** shows an even more striking

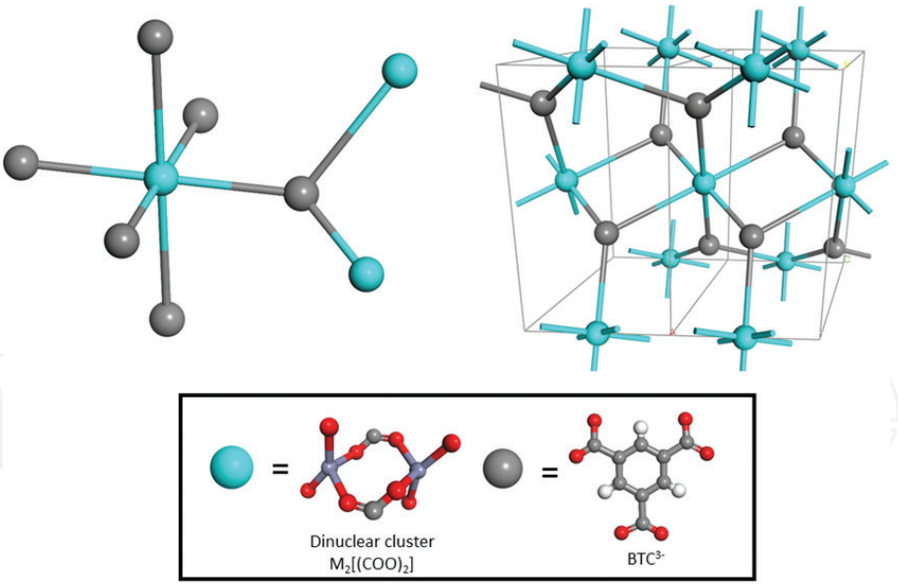

Figure 7.
The structure represents (3,6)-connected network. This corresponds to the following formulas: [BMI][Zn(BTC)] (FUTZEB), and $[EMI]_2[In_2Co(OH)_2(BTC)_2Br_2]$ (VUVZAP).

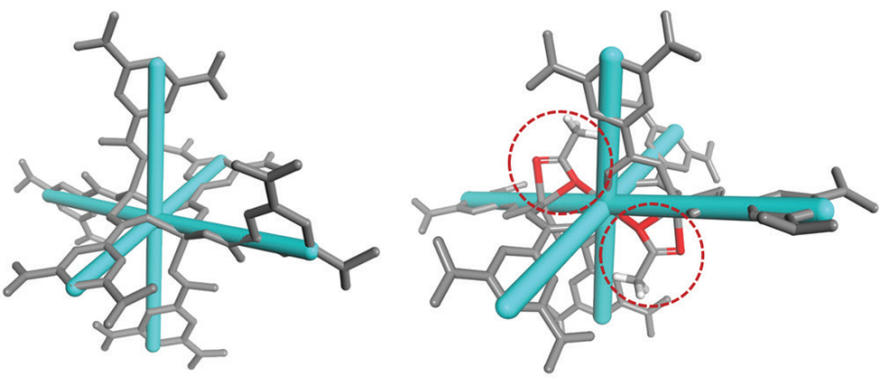

Figure 8.
The left is the [RMI][Metal(BTC)] class with binuclear clusters and the right $[RMI]_2[Metal_3(HBTC)_4(H_2O)]$ with trinuclear clusters. Light blue stick represents the octahedral connections between metal clusters and BTC to better illustrate the topological identity of the two groups. The molecular moieties in the red circle represent acetate groups.

example with [RMI][Metal(BTC)] structure and $[RMI]_2[M_3(HBTC)_4(H_2O)]$ structure. Although it is very difficult to catch any similarities from the formula nor the structure if at first glance they actually fall under the same topology umbrella. This remarkable similarity is possible because some coordination sites of the trinuclear metal cluster are occupied by another molecular moiety, OAc in this case as shown in **Figure 7**. These places the trinuclear clusters in the octahedral coordination mode, which is the maximum coordination that binuclear metal clusters can have.

5. Outstanding properties of ionothermally prepared MOFs

In previous sections, we have explored through the diverse structures prepared by ionothermal synthesis and several perspectives through which the groups of structures may be analysed to gain deeper insights. The last step is to find a practical use for those insights. The versatility of ionothermal synthesis, that its reaction environment may be easily altered and related to the change in products, directly

leads us towards the diversity of structures that may be prepared through the methodology. As such, ionothermal synthesis promises a variety of potential uses, although most of them have obstacles yet to be resolved along the way towards practical employment.

5.1 Ion exchange is the key to make use of the pores

Many of the most popularly studied application of MOFs make use of the frameworks as molecular sieves. The nanoscale pores of MOFs can selectively filter out any chemicals that do not fit into them and this selectivity can be chosen by the industry among the diversity of reported structures. The first use of ionothermally prepared MOFs is probably also the same. In this case, ionothermal synthesis has one advantage that the solvent functions as a template and can be varied in size to modify the pore size. However, it is a double-edged sword that actually limits the practicality of ionothermal synthesis. To make any use of the pores, the templates occupying the pores must be removed. The problem is that they hardly ever do.

The void volume of the structures synthesised with the cation varied in size has been compared in **Tables 4**, **5** and **7**. Frameworks with the solvent resident in their channels, or cavities, tend to have compact structure with the void volume as low as 0% of the unit cell volume. For your reference, MOF-5, a representative framework, has a void cavity as large as 70% of unit cell volume. This absence of void volume arose because of the large solvent cations stuck in the cavity, rather than the framework itself. When calculated with the resident cations completely removed, void volume was increased to approximately 50% of unit cell volume. In theory, the large volume occupied by the cations may be decreased by subjecting the framework to ion exchange with smaller cations, so that the rest may be used purposefully. Unfortunately for now, this possibility seems to stay only in theory. Given its important position—the first step in bringing ionothermal synthesis to practicality, tremendous efforts have been put into making this exchange possible, but they rarely succeeded. In one case that we tested, evacuation of cations was observed in $[BMI]_2[Co_2(BTC)_2(H_2O)_2]$ crystals upon treatment with water, but only when accompanied with significant destruction of the framework [31]. Nevertheless, Li et al. reported partial but stable ion exchange with $[EMI]_2[In_2Co(OH)_2(BTC)_2Br_2]$ crystals [32], suggesting a new possibility for the ionothermal synthesis methodology.

5.2 Placing metal atoms in proximity to yield novel characteristics

The limitations posed by the irreplaceable templates have indeed disappointed the researchers and presumably many of you, too. However, even if the pores of ionothermally prepared MOFs are totally unusable, they still have some valuable characteristics. It is very common in the world of nanoscience that a substance acquires some characteristics completely different from those of its macroscopic bulk. One of the most frequently reported application is detection of chemicals via photoluminescence that changes upon encounter with specific chemicals. This includes the photoluminescence of europium ions in $[HMI][Eu(DHBDC)_{2,}$ where DHBDC indicates 2,5-dihydroxytelephtalic acid, capable of detect Ba^{2+} ions quantitatively [25], and $[RMI][Eu_2(BDC)_3Cl]$ for detection of aniline [18]. In addition, ionothermally prepared $[EMI][Dy_3(BDC)_5]$, a rod-shaped polymer, has been shown to exhibit slow magnetic relaxation behaviour like single-molecule magnets [22]. It seems like ionothermally prepared structures may be applied for any purposes that exist in the field of nanochemistry.

6. Conclusion

In a system of different chemical outcomes from related starting conditions, it is often difficult to track what has caused that difference. The ionothermal synthesis methodology is excellent in this aspect. Changes can be made in a gradual and continuous manner to observe how the result reacts to them. By organising the results based on their solvents, we can connect the dots to find useful correlations that can be both used for intra- and extrapolation. The relations are often very intuitive. For this simplicity to not lead to inaccuracy, there is a need to carefully examine the frameworks and how they react with the reaction environment—the ionic liquid that functions both as solvent and template. In the course of simplifying the frameworks for examination follows merging of structures into large topology groups, which can be used to better organise once separated correlations from various chemical systems. Despite of all the positive characters of ionothermal synthesis, however, there is a limit to their practical application—the irreplaceable reaction templates. For this rich and potentially richer field of material synthesis to contribute to the industry, efforts must be made to either resolve the issue or to find uses from the framework itself, rather than the voids.

List of abbreviations

Cations

RMI	1-alkyl-3-methylimidazolium
EMI	1-ethyl-3-methylimidazolium
PMI	1-propyl-3-methylimidazolium
BMI	1-butyl-3-methylimidazolium
PEMI	1-pentyl-3-methylimidazolium
HMI	1-hexyl-3-methylimidazolium

Organic ligands

BTC	1,3,5-benzenetricarboxylic acid
BDC	1,4-benzene dicarboxylic acid
NDC	1,4-naphthalene dicarboxylic acid
4,4′-bpy	4,4′-bipyridine
DHBDC	2,5-dihydroxytelephtalic acid

Others

MOF	metal organic framework
CSD	Cambridge structural database
PXRD	powder X-ray diffraction
OAc	acetate
CCDC	Cambridge crystallographic data centre

Author details

Hyun-Chang Oh[1], Sukwoo Jung[2], Il-Ju Ko[1] and Eun-Young Choi[1,2]*

1 Department of Chemistry, KAIST, Daejeon, Republic of Korea

2 Department of Chemistry and Biology, Korea Science Academy of KAIST, Busan, Republic of Korea

*Address all correspondence to: faujasite1@kaist.ac.kr

IntechOpen

References

[1] Xu L, Yan S, Choi E-Y, Lee JY, Kwon Y-U. Product control by halide ions of ionic liquids in the ionothermal syntheses of Ni-(H)BTC metal-organic frameworks. Chemical Communications. 2009:3431-3433

[2] Jin K et al. [Cu(i)(bpp)]BF4: The first extended coordination network prepared solvothermally in an ionic liquid solvent. Chemical Communications. 2002:2872-2873

[3] Morris RE, Weigel SJ. The synthesis of molecular sieves from non-aqueous solvents. Chemical Society Reviews. 1997;**26**:309-317

[4] Del Pópolo MG, Voth GA. On the structure and dynamics of ionic liquids. The Journal of Physical Chemistry. B. 2004;**108**:1744-1752

[5] Rogers RD, Seddon KR. Ionic liquids—solvents of the future? Science. 2003;**302**:792-793

[6] Earle MJ et al. The distillation and volatility of ionic liquids. Nature. 2006;**439**:831-834

[7] Hyun Chang O, Sukwoo J, Ko I-J, Eun Young C. Tabular organisation of ionothermally prepared MOFs to extrapolate chemical trends and successfully predict synthesis results. Biomedical Journal of Scientific & Technical Research. 2018). BJSTR. MS.ID.000996;**4**(1):4. DOI: 10.26717/BJSTR.2018.04.000996

[8] Plechkova NV, Seddon KR. Ionic liquids: "Designer" solvent for green chemistry. In: Tundo P, Perosa A, Zecchini F, editors. Methods and Reagents for Green Chemistry. Wiley. 2007. DOI: 10.1002/9780470124086.ch5

[9] Tokuda H, Hayamizu K, Ishii K, Susan MABH, Watanabe M. Physicochemical properties and structures of room temperature ionic liquids. 2. Variation of alkyl chain length in imidazolium cation. The Journal of Physical Chemistry. B. 2005;**109**:6103-6110

[10] Xu L, Kwon Y-U, de Castro B, Cunha-Silva L. Novel Mn(II)-based metal-Organic frameworks isolated in ionic liquids. Crystal Growth & Design. 2013;**13**:1260-1266

[11] Parnham ER, Morris RE. Ionothermal synthesis of zeolites, metal-organic frameworks, and inorganic-organic hybrids. Accounts of Chemical Research. 2007;**40**:1005-1013

[12] Xu L, Choi EY, Kwon YU. Combination effects of cation and anion of ionic liquids on the cadmium metal-organic frameworks in ionothermal systems. Inorganic Chemistry. 2008;**47**:1907-1909

[13] Liao J-H, Wu P-C, Huang W-C. Ionic liquid as solvent for the synthesis and crystallization of a coordination polymer: (EMI)[Cd(BTC)] (EMI = 1-Ethyl-3-methylimidazolium, BTC = 1,3,5-benzenetricarboxylate). Crystal Growth & Design. 2006;**6**:1062-1063

[14] Zhang Z-H, Xu L, Jiao H. Ionothermal synthesis, structures, properties of cobalt-1,4-benzenedicarboxylate metal–organic frameworks. Journal of Solid State Chemistry. 2016;**238**:217-222

[15] Xu L et al. The influence of 1-alkyl-3-methyl imidazolium ionic liquids on a series of cobalt-1,4-benzenedicarboxylate metal–organic frameworks. CrystEngComm. 2014;**16**:10649-10657

[16] Tapala W, Prior TJ, Rujiwatra A. Two-dimensional anionic zinc

benzenedicarboxylates: Ionothermal syntheses, structures, properties and structural transformation. Polyhedron. 2014;**68**:241-248

[17] Zhang Z-H, Liu B, Xu L, Jiao H. Combination effect of ionic liquid components on the structure and properties in 1,4-benzenedicarboxylate based zinc metal–organic frameworks. Dalton Transactions. 2015;**44**:17980-17989

[18] Feng H-J, Xu L, Liu B, Jiao H. Europium metal-organic frameworks as recyclable and selective turn-off fluorescent sensors for aniline detection. Dalton Transactions. 2016;**45**:17392-17400

[19] Cao HY et al. Ionothermal syntheses, crystal structures and luminescence of three three-dimensional lanthanide-1,4-benzenedicarboxylate frameworks. Inorganica Chimica Acta. 2014;**414**:226-233

[20] Huang G, Yang P, Wang N, Wu JZ, Yu Y. First lanthanide coordination polymers with N,N-dimethylformamide hydrolysis induced formate ligands. Inorganica Chimica Acta. 2012;**384**:333-339

[21] Li S-Y, Du L, Liu Z-H. Ionothermal synthesis, crystal structure, and luminescent properties of two novel layered indium-1,4-benzenedicarboxylate complexes. Synthesis and Reactivity in Inorganic, Metal-Organic, and Nano-Metal Chemistry. 2016;**46**:675-680

[22] Liu Q-Y et al. Ionothermal synthesis of a 3D dysprosium-1,4-benzenedicarboxylate framework based on the 1D rod-shaped dysprosium-carboxylate building blocks exhibiting slow magnetization relaxation. CrystEngComm. 2014;**16**:486-491

[23] Liao J-H, Huang W-C. Ionic liquid as reaction medium for the synthesis and crystallization of a metal-organic framework: $(BMIM)_2[Cd_3(BDC)_3Br_2]$ (BMIM=1-butyl-3-methylimidazolium, BDC=1,4-benzenedicarboxylate). Inorganic Chemistry Communications. 2006;**9**:1227-1231

[24] Xiahou Z-J, Wang Y-L, Liu Q-Y, Wei J-J, Chen L-L. Ionothermal synthesis of a 3D heterometallic coordination polymer based on the rod shaped copper(II)–sodium(I)-carboxylate secondary building units with a pcu topology. Inorganic Chemistry Communications. 2013;**38**:62-64

[25] Lin Z, Wragg DS, Morris RE. Microwave-assisted synthesis of anionic metal–organic frameworks under ionothermal conditions. Chemical Communications. 2006:2021-2023. DOI: 10.1039/B600814C

[26] Lin Z, Slawin AMZ, Morris RE. Chiral induction in the ionothermal synthesis of a 3-D coordination polymer. Journal of the American Chemical Society. 2007;**129**:4880-4881

[27] Xu L, Choi E-Y, Kwon Y-U. A new 3D nickel(II) framework composed of large rings: Ionothermal synthesis and crystal structure. Journal of Solid State Chemistry. 2008;**181**:3185-3188

[28] Lin Z, Li Y, Slawin AMZ, Morris RE. Hydrogen-bond-directing effect in the ionothermal synthesis of metal coordination polymers. Dalton Transactions. 2008:3989-3994. DOI: 10.1039/b802892c

[29] Lin Z, Wragg DS, Warren JE, Morris RE. Anion control in the ionothermal synthesis of coordination polymers. Journal of the American Chemical Society. 2007;**129**:10334-10335

[30] Wang YL et al. Ionothermal syntheses and crystal structures of

two cobalt(II)-carboxylate compounds with different topology. Inorganic Chemistry Communications. 2011;**14**:380-383

[31] Ko IJ, Oh HC, Cha YJ, Han CH, Choi EY. Ionothermal synthesis of a novel 3D cobalt coordination polymer with a uniquely reported framework: $[BMI]_2[Co_2(BTC)_2(H_2O)_2]$. Advances in Materials Science and Engineering. 2017;**2017**:6

[32] Li SY, Liu ZH. Synthesis, structure and property of a 3D heterometallic complex constructed by trinuclear $[In_2Co(OH)_2(COO)_4]$ cluster and BTC ligand. Journal of Cluster Science. 2015;**26**:1959-1970

[33] Xu L, Choi EY, Kwon YU. Ionothermal synthesis of 3D zinc coordination polymer: $[Zn_2(BTC)(OH)(I)](BMIM)$ containing novel tetra nuclear building unit. Inorganic Chemistry Communications. 2008;**11**:150-154

[34] Xu L, Choi EY, Kwon YU. Ionothermal syntheses of six three-dimensional zinc metal-organic frameworks with 1-alkyl-3-methylimidazolium bromide ionic liquids as solvents. Inorganic Chemistry. 2007;**46**:10670-10680

[35] Xu L, Choi EY, Kwon YU. Ionothermal synthesis of a 3D Zn-BTC metal-organic framework with distorted tetranuclear $[Zn_4(\mu_4\text{-}O)]$ subunits. Inorganic Chemistry Communications. 2008;**11**:1190-1193

[36] Ordonez C, Fonari M, Lindline J, Wei Q, Timofeeva T. How structure-directing cations tune the fluorescence of metal-organic frameworks. Crystal Growth & Design. 2014;**14**:5452-5465

[37] An B, Wang J-L, Bai Y, Dang D-B. Systematic design of secondary building units by an efficient cation-directing strategy under regular vibrations of ionic liquids. Dalton Transactions. 2015;**44**:14666-14672

[38] Gao MJ, Wang YL, Cao HY, Liu QY, Chen LL. Ionothermal syntheses, crystal structures and luminescence of two lanthanide-carboxylate frameworks based on the 1, 4-naphthalenedicarboxylate and oxalate mixed ligands. Zeitschrift für anorganische und allgemeine Chemie. 2014;**640**:2472-2476

[39] Tan B et al. Ionothermal syntheses, crystal structures and properties of three-dimensional rare earth metal-organic frameworks with 1,4-naphthalenedicarboxylic acid. Dalton Transactions. 2012;**41**:10576-10584

[40] Wu ZF, Hu B, Feng ML, Huang XY, Zhao YB. Ionothermal synthesis and crystal structure of a magnesium metal-organic framework. Inorganic Chemistry Communications. 2011;**14**:1132-1135

[41] Wu Z-F et al. An ionothermally synthesized Mg-based coordination polymer as a precursor for preparing porous carbons. CrystEngComm. 2015;**17**:4288-4292

[42] Wei JJ, Liu QY, Wang YL, Zhang N, Wang WF. Ionothermal synthesis of a 3D zinc(II)-carboxylate coordination polymer with bcu topology based on heptanuclear $[Zn_7(\mu_4\text{-}O)_2]$ cluster. Inorganic Chemistry Communications. 2012;**15**:61-64

[43] An B, Bai Y, Wang J-L, Dang D-B. Cation-size-controlled assembly of the Ni(Ac)2-1, 4-H2NDC system: Geminal dicationic ionothermal syntheses, crystal structures and magnetic properties. Dalton Transactions. 2014;**43**:12828-12831

[44] Tan B, Xie ZL, Huang XY, Xiao XR. Ionothermal synthesis, crystal

structure, and properties of an anionic two-dimensional cadmium metal organic framework based on paddle wheel-like cluster. Inorganic Chemistry Communications. 2011;**14**:1001-1003

[45] Liu SS, Cheng M, Li B. Ionothermal Synthesis of a 3D Luminescent Strontium(∏) Coordination Polymer with Dodecanuclear Metallocylclic Ring Segments. Journal of Inorganic and Organometallic Polymers. 2015;**25**:1103-1110